Journal of Sound and Vibration (2000) **235**(3), 477–494
doi:10.1006/jsvi.2000.2945, available online at http://www.idealibrary.com on IDEAL®

DESIGN OPTIMIZATION OF MARINE ENGINE–MOUNT SYSTEM

J. S. Tao, G. R. Liu and K. Y. Lam

Institute of High Performance Computing, 89-*C Science Park Drive* #02-11/12, *The Rutherford*, *Singapore* 118261, *Singapore. E-mail*: *hpctaojs@nus.edu.sg*

(*Received* 9 *December* 1999, *and in final form* 7 *March* 2000)

Design optimization of marine engine–mount system for vibration control is presented in this paper. The engine is modelled as a rigid body with supports connected to a rigid floor. The mounts are modelled as three-dimensional isolators with hysteresis damping. The objective is to select the stiffness coefficient and orientations of individual mount in order to minimize the vertical force transmitted from the engine to the floor to control the structure-borne noise. Constraints are imposed to keep the isolator static and dynamic deflection within the desired limits and a minimum gap between system natural frequency and engine excitation frequency for avoiding possible system resonance. The sequential quadratic programming (SQP) technique has been applied as the optimization algorithm. The typical force and moment of a 4-stroke engine with one cylinder is analyzed and input in the optimization system. The results of optimization are compared with that of a conventional engineering design with the isolators working under their maximum allowable deflection. This comparison shows that, as compared with force transmission of the conventional isolation system, the value of optimized system is only half for multi-frequencies excitation and one-fourth for single frequency excitation. The mechanism of vibration isolation involved in the optimization is investigated with the frequency response of the system. Sensitivity study of the system with the variation of the design parameters is also carried out and proves that the minimum obtained is the global value in the range of design parameters.

1. INTRODUCTION

Vibration isolation of marine engine on compliant mounts is a very common and important engineering design problem. The challenge for the design engineer is how to select the vibration isolators and how to properly install them in order to minimize the structure-borne noise and vibration level in the cabins or noise breakout into the water which is especially critical for warships. Unlike in the normal application in the building, a mounting system for marine engine should be able to react the strong dynamic force caused by wave slap, cornering loads, and docking impact. Thus, the static deflection of isolators shall be designed within a limit for keeping the balance of engine under the strong impact. This will increase the vibration transmitted into the hull structure and challenge the design engineer to create even more effective mounting system. One useful method for helping the design engineer to develop more effective mounting systems is through optimization techniques.

Many researchers have involved in the study of this area. Sevin *et al.* [1] summarized some achievements by 1971. However, due to the limitation of computational power, most of work has been done at that time concentrated on the theoretical analyses and

0022-460X/00/330477 + 18 $35.00/0

single-degree-of-freedom (d.o.f.) systems. Recently, due to the rapid development of the computational technology, this area attracts more attention. Spiekermann *et al.* [2] used the penalty function optimization method to obtain optimal design of engine mounting in automobile application by moving six system natural frequencies away from engine excitation frequency. This function penalized the natural frequencies in an undesirable frequency range and also large design changes. However, Swanson *et al.* [3] showed that the transmitted forces should be directly minimized rather than the natural frequencies in order to determine a "truly" optimal design of the mount. He used the recursive quadratic programming technique for the optimal isolation system design of aircraft engine. The objective function in his study is the total force transmitted to the structure, and the design variables are the stiffness of the mounts. The constraint is the dynamic deflection of c.g of engine. Ashrafliuon [4] continued Swanson's study but with more design variables and a flexible base. Snyman *et al.* [5] carried out another study to minimize the total force transmitted to the base by optimizing the balancing mass and associated phase angles of a V-engine. No constraint is imposed in his study.

In summary, the previous studies on the optimization of engine mounting systems mainly focused on two aspects; One is to minimize the transmitted force by moving the system natural frequencies away from an undesired frequency; the other is to directly optimize the force transmission by adjusting the design parameters. There is no report on the theoretical analyses of the objective function and sensitivity study of their optimization results. It is possible that the minimum value obtained in their studies is at the anti-resonance point with system frequencies quite near the excitation frequencies. Harris *et al.* [6] present the frequency response of a resiliently supported rigid body under the excitation of force and moment. It is clearly indicated that there is an anti-resonance frequency between two natural frequencies of the system. The small shift of the system variables may cause a resonance of the system and thus totally destroy the initial purpose. On the other hand, the objective function in their study is the total force transmitted to the structure. However, the structure-borne noise or vibration level transmitted to other spaces significantly depends on the vertical force (normal to the floor) which generates the bending wave in the structure. Also, the previous studies concentrated on the system with a single frequency excitation due to a rotating unbalance. However, the excitation force of an engine is normally complicated and with multi-frequencies excitation. It can be anticipated that the optimization results should be quite different.

In the present study, the vibration isolation system of an engine is optimized by using sequential quadratic programming (SQP) technique. The mounting stiffness and orientation of isolators are chosen as the design variables. The objective function to be minimized is the summation of the transmitted force normal to the base at all mounting positions. To avoid the selection with excitation frequencies too near to the system resonance frequencies, a minimum gap between them is set as a constraint condition in the optimization. The other constraint conditions in the optimization are set to limit the static and dynamic response of isolators under the excitation and also to meet the balancing requirement of the engine installation. An example of a 4-stroke engine with one cylinder is used to show that the optimization technique is effective. The optimization results are compared with that of a conventional engineering design with all isolators working under their maximum allowable static deflection. The mechanism of the vibration attenuation by optimization is investigated based on the frequency response of objective function and compared with that of the conventional design. Sensitivity study of the system with the variation of the design parameters is also carried out and it proves that the minimum obtained is the global value in the range of bounds of design parameters.

2. ENGINE–MOUNT SYSTEM EQUATIONS

The engine is modelled as a rigid body that is supported by four vibration isolators fixed to a rigid floor as showed in Figure 1. A rigid-body model is suitable for a structure whose geometry points remains fixed relative to one another [2]. The right-hand global co-ordinate system $Gxyz$ has its origin at the centre of mass of the engine when in static equilibrium. The three orthogonal co-ordinate axes, which are shown in Figure 1, are set with Y, Z-axis parallel to the floor and X normal to the floor. The crank-shaft of engine is in the direction of Z-axis. The rigid-body model consists of six DOFs that include three translation and three rotation modes respectively. Under the assumption of "small" motion, the engine–mount system equation can be written as

$$[\mathbf{M}]\{\ddot{\mathbf{x}}\} + [\mathbf{K}]\{\mathbf{x}\} = \{\mathbf{F}\}e^{i\omega t}, \tag{1}$$

where $[\mathbf{M}]$ is the 6×6 engine's rigid mass matrix; $\{\mathbf{x}^T\} = [x_g \ y_g \ z_g \ \theta_x \ \theta_y \ \theta_z]$ is the displacement vector at c.g of engine, $[\mathbf{K}]$ is the 6×6 stiffness matrix, $\{\mathbf{F}\}$ is the 6×1 vector of excitation forces and moments and ω is the forcing angular frequency.

The majority of mounts used in the marine engine mounting are of a rubber bonded to metal, or elastomeric construction. Complex spring stiffness is used to model the dynamic behaviour of the mount [3]. The complex stiffness of a mount in the three directions of its local co-ordinate system is defined by the equation

$$[\mathbf{k}'] = [\mathbf{k}](1 + j\eta), \tag{2}$$

where η is the loss factor and $j = \sqrt{-1}$. The stiffness matrix must be transformed from its local mount co-ordinate system to the global co-ordinate system situated at the engine c.g.

The stiffness in the global co-ordinate system can be expressed as

$$\{\mathbf{k}_i\} = [\mathbf{A}]\{\mathbf{k}'\}[\mathbf{A}^{-1}], \tag{3}$$

where $[\mathbf{A}]$ is transpose matrix of the Euler angle matrix [7] and can be written as

$$[\mathbf{A}] = \begin{bmatrix} \cos\alpha\cos\beta & -\sin\alpha\cos\gamma + \cos\alpha\sin\beta\sin\gamma & \sin\alpha\sin\gamma + \cos\alpha\sin\beta\cos\gamma \\ \sin\alpha\cos\beta & \cos\alpha\cos\gamma + \sin\alpha\sin\beta\sin\gamma & -\cos\alpha\sin\gamma + \sin\alpha\sin\beta\cos\gamma \\ -\sin\beta & \cos\beta\sin\gamma & \cos\beta\cos\gamma \end{bmatrix}. \tag{4}$$

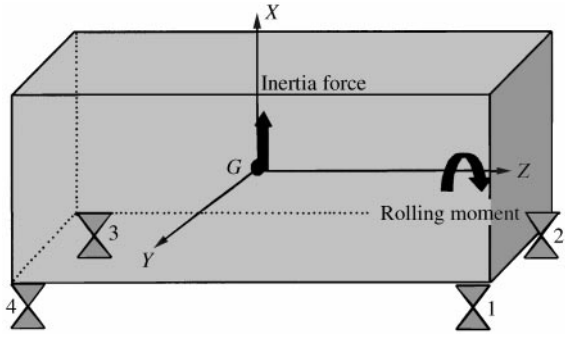

Figure 1. Rigid body on compliant mounts. The origin of global co-ordinate system is at the centre of gravity of engine. Y- and Z-axis are parallel to the floor and X-axis is normal to the floor.

In the above transformation, the first is a rotation through an angle α about the Z-axis, followed by the second rotation through an angle β about Y-axis, and then final rotation through γ about X-axis.

The stiffness matrix [**K**] can be calculated [6] based on the stiffness matrix [$\mathbf{k}_i$] in equation (3) and position matrix [$\mathbf{r}_i$] of individual mount i. The displacement vector $\{\mathbf{x}\}$ in equation (1) is thus expressed as

$$\{\mathbf{x}\} = \{\mathbf{F}\}/([\mathbf{K}] - \omega^2[\mathbf{M}]). \tag{5}$$

The displacement at each mount is

$$U_{xi} = x_g + X_i\theta_y - Y_i\theta_z, \tag{6}$$

$$U_{yi} = y_g - Z_i\theta_x + X_i\theta_z, \tag{7}$$

$$U_{zi} = z_g - X_i\theta_y + Y_i\theta_x, \tag{8}$$

where X_i, Y_i, and Z_i are the co-ordinates of ith mount at global co-ordinate system.

The force transmitted to the floor at each mount in three directions can be written as

$$\{\bar{\mathbf{F}}_i\} = -[\mathbf{k}_i]\{\mathbf{U}_i\}. \tag{9}$$

The total force transmitted to the floor at all mounts is

$$\bar{F} = \sum_{i=1}^{N} (\bar{F}_{xi}^2 + \bar{F}_{yi}^2 + \bar{F}_{zi}^2)^{1/2}. \tag{10}$$

The total force transmitted to the floor in the vertical direction of all mounts is

$$\bar{F}_x = \sum_{i=1}^{N} |\bar{F}_{xi}|. \tag{11}$$

F_x and F are the force under the excitation angular frequency ω. In the case of excitation force with multi-frequencies (ω_j), the force F and F_x are expressed as

$$\bar{F} = \sum_{j=1}^{n} \bar{F}_{\omega j}, \tag{12}$$

$$\bar{F}_x = \sum_{j=1}^{n} \bar{F}_{x\omega j}. \tag{13}$$

3. FORCE AND MOMENT EXERTED BY THE ENGINE

The shaking force and moment of an engine have been detailed investigated by Paul [8]. A single cylinder engine model of Paul is illustrated in Figure 2. After balancing of the rotating mass and with constant crank angular velocity ω, for an engine with one cylinder, there have only inertia force in the vertical direction and rolling moment in the crank-shaft

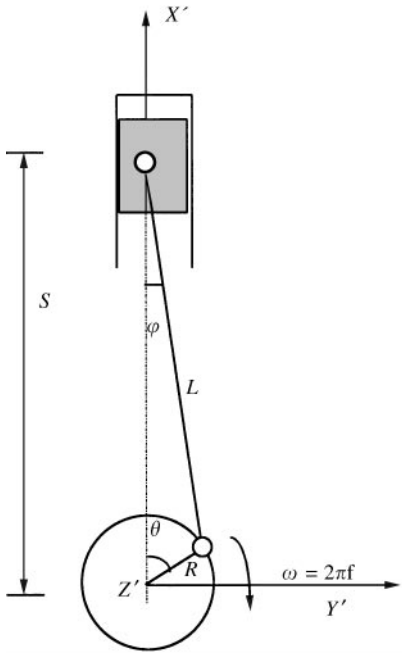

Figure 2. Single cylinder engine model.

direction. The force and moment in its local co-ordinate system (X', Y', Z') as shown in Figure 2 can be expressed as

$$F'_x = (m_{rot} + m_{rec})R\omega^2 + m_{rec}R\omega^2(A_2 \cos 2\theta - A_4 \cos 4\theta + A_6 \cos 6\theta - \cdots), \tag{14}$$

$$M'_z = (P + m_{rec}\ddot{s})s \tan \varphi, \tag{15}$$

where m_{rot} is the rotation mass, m_{rec} is the reciprocating mass, s, θ, R and φ are illustrated in Figure 2. P is the gas force inside the cylinder that can be calculated based on the gas pressure and compression ratio of engine [8]. Typical frequency spectra of F'_x and M'_z are calculated and illustrated in Figure 3 where (a) is the vertical inertia force and (b) is the rolling moment. It is found that the disturbing frequencies are at f and $2f$ for inertia force in Figure 3(a) but at $1/2f$, f, $3/2f$ and $2f$ for rolling moment in Figure 3(b). Here, f is the running frequency of engine which equals to angular velocity ω divided by 60.

The forces and moments above are based on the local co-ordinate system on the crank-shaft and cylinder as shown in Figure 2. These forces and moments should be transformed to the values in the global co-ordinate system with the origin at the centre of gravity of engine. The force transformation can be expressed as

$$\begin{bmatrix} F_x \\ F_y \\ F_z \end{bmatrix} = [\mathbf{A}^{-1}] \begin{bmatrix} F'_x \\ F'_y \\ F'_z \end{bmatrix}, \tag{16}$$

where $[\mathbf{A}]$ is transformation matrix as defined in equation (4).

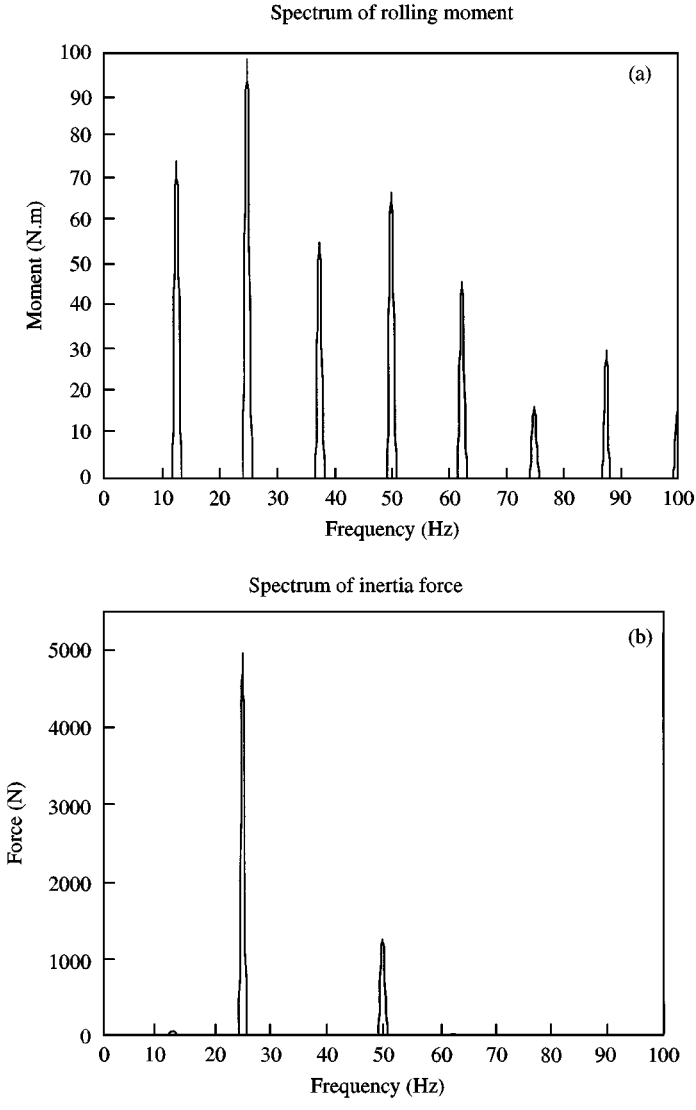

Figure 3. Spectra of excitation force and moment of a 4-stroke engine with one cylinder. (a) is the spectrum of moment around Z'-axis. (b) is the spectrum of force in the X' direction.

The moments generated by the force $F'_x,\ F'_y,\ F'_z$ in the global co-ordinate systems can be expressed as

$$\vec{\mathbf{M}}_f = \vec{\mathbf{r}} \times \vec{\mathbf{F}} = [\mathbf{r}]\vec{\mathbf{r}}_G \times [\mathbf{F}]\vec{\mathbf{r}}_G = ([\mathbf{A}^{-1}][\mathbf{r}_0])\vec{\mathbf{r}}_G \times ([\mathbf{A}^{-1}][\mathbf{F}'])\vec{\mathbf{r}}_G = [\mathbf{A}^{-1}] \begin{bmatrix} F'_z y_0 - F'_y z_0 \\ F'_x z_0 - F'_z x_0 \\ F'_y x_0 - F'_x y_0 \end{bmatrix} \vec{\mathbf{r}}_G, \quad (17)$$

where $\vec{\mathbf{r}}_G = [\vec{\mathbf{i}}, \vec{\mathbf{j}}, \vec{\mathbf{k}}]$ is the unit vector of global co-ordinate system. $\vec{\mathbf{r}} = [x, y, z]\vec{\mathbf{r}}_G$ is the displacement vector from the origin of global co-ordinate system to the point of force.

$\vec{\mathbf{F}} = [F_x, F_y, F_z]\vec{\mathbf{r}}_G$ is the force vector in the global co-ordinate system. $[\mathbf{r}_0] = [x_0, y_0, z_0]^{\mathrm{T}}$ is the translational displacement matrix from the origin of global co-ordinate system to that of the local co-ordinate system since the force point is considered at the origin of the local co-ordinate system. The transformation of the moments in the local co-ordinate system to that in the global co-ordinate system can be expressed as

$$\vec{\mathbf{M}}_M = \vec{\mathbf{r}} \times \vec{\mathbf{F}} = [\mathbf{r}]\vec{\mathbf{r}}_G \times [\mathbf{F}]\vec{\mathbf{r}}_G = ([\mathbf{A}^{-1}][\mathbf{r}'])\vec{\mathbf{r}}_G \times ([\mathbf{A}^{-1}][\mathbf{F}'])\vec{\mathbf{r}}_G = [\mathbf{A}^{-1}]\begin{bmatrix} M'_x \\ M'_y \\ M'_z \end{bmatrix}\vec{\mathbf{r}}_G, \quad (18)$$

where $[\mathbf{r}']$ is the displacement matrix from the origin of local co-ordinate system to the point of force in the local system. In the case that $[\mathbf{A}]$ equals a unity matrix where no rotation exists between two co-ordinate systems, the moments keep the same after the transformation.

Figure 4(a–f) illustrates the spectra after the transformation of the force and moment in Figure 3. The rotation angles α, β, γ equal to 5°, 10° and 15° respectively. The translation distances between two co-ordinate systems are 0·02 m, 0·03 m and 0·1 m respectively.

4. OPTIMIZATION

Optimization problem is concerned with the minimization of a objective function $F(\mathbf{a})$ that may be subject to a number of constraints or bounds. It can be expressed as

$$\text{Minimize} \quad F(\mathbf{a}) \quad (19)$$

subject to

$$G_i(\mathbf{a}) = 0 \quad i = 1, \ldots, m, \qquad \text{equity constraint,} \quad (20)$$

$$G_i(\mathbf{a}) \leqslant 0 \quad i = m+1, \ldots, n, \qquad \text{inequity constraint,} \quad (21)$$

$$\mathbf{a}_l \leqslant \mathbf{a} \leqslant \mathbf{a}_u, \qquad \text{bounds of variables,} \quad (22)$$

where $F(\mathbf{a})$ is the objective function, $\mathbf{a}$ is the design parameter vector, $\mathbf{a}_l$ is the lower bound of variables while $\mathbf{a}_u$ is the upper bound of the design variables and n is the total number of constraints.

The objective function here is the total force in the direction normal to the installation base rather than the total force in all directions as applied by Ashrafiuon [4] and Snyman *et al.* [5]. This is because only the force normal to the base can excite the bending wave which contributes most of energy of structure-borne noise.

The inequity constraint, called "dynamic constraint", is imposed to limit the maximum allowable dynamic displacement at each mount in three directions and expressed as

$$|\mathbf{U}_i| \leqslant c_1, \quad (23)$$

where $\mathbf{U}_i$ is the displacement vector at ith mount and c_1 is the "dynamic constraint". This is critical at low frequency where a large displacement happens. The limits on the

displacement of the c.g of engine as applied by Ashrafiuon [4] cannot reflect the situation at each mount.

It is possible that the optimization result may be at the point where the system resonance frequency is just beside the excitation frequency. This often happens at the anti-resonance point. In this case, a small change of design parameters may cause the amplification of excitation force rather than the attenuation. Thus, another inequity constraints, called "frequency constraint", must be imposed to set a minimum gap between excitation frequencies and system resonance frequencies and expressed as

$$|f_j - \mathbf{f}_n| \leqslant c_2, \tag{24}$$

where f_j is the selected excitation frequency, $\mathbf{f}_n$ is the natural frequency vector, c_2 is the "frequency constraint", c_2 should not be too large otherwise it is difficult to find a feasible solution with optimization, and also not all the excitation frequencies are selected as f_j. Normally, f_j is selected at two or three excitation frequencies where with most of excitation energy.

The equity constraints are imposed to limit the orientation of isolator. It is used to keep as best the same static loading of all mounts in three directions. This will decrease the risk of losing balance of engine under the strong impact.

The design variables under present study include the stiffness and orientation of the isolator. The lower bound $\mathbf{a}_l$ for stiffness is imposed to limit the maximum allowable static deflection. This is critical for the stability of engine under the impact force. The upper bound $\mathbf{a}_u$ for stiffness is imposed to control the "wave" effect of isolation system [6]. This is because, as the stiffness of the mounting system increases, so does the natural frequencies of the system, it will become more apparent that the system behaves like a distributed system. The lower bound for the orientation angle of isolator is zero, which means the coincidence of local co-ordinate system with global co-ordinate system. The upper bound of orientation angle is 90° that means the isolator is always under compression rather than suspension. This is the requirement of most of the marine engine installation.

To the optimization algorithms, the genetic algorithms, which were recently introduced for optimization [9, 10], were considered in the beginning. The big advantage of this method is that it undertakes a wider search in the entire design variable space than the conventional gradient-based algorithms. This is mainly due to the random character of the procreation process in the genetic operators. This wider searching increases the probability of converging to a global minimum. However, due to the random character of search process, genetic optimization requires a huge amount of useless objective function evaluations and thus a long computer time. Fonseca [11] indicated that the best gradient-based algorithms even produces a better and faster solution than the best genetic algorithm in a similar amount of computational time. Pogu *et al.* [12] considered genetic algorithm and other random search technique only as "last resort" methods for solving continuous optimization problems. Sequential quadratic programming algorithm is considered as a superior method in the conventional gradient-based algorithms for solving non-linear constrained optimization problems in terms of computer time and number of function evaluations [13, 14] and thus is selected in the present study. This technique is also selected by some distinguished commercial software like Pantran/Nastran [15] and Matlab [16]. In SQP, the objective and constraint functions are approximated using Taylor series approximations. However, a quadratic, rather than a linear approximation of objective function is used which also becomes the part of the name of SQP. The optimization problem is thus approximated by a quadratic programming (QP) problem at each iteration. This QP sub-program is solved using a standard QP solver. The problem terminates if the

minimum is reached and all constraints are satisfied. If not, the solution of QP guarantees that the further descend is possible and approximation process repeats. An overview of SQP is found in Fletcher [17].

SQP method may not able to find a global minimum. This is due to the factors that all the conventional gradient-based algorithms are based upon the functions with continuous first and second derivatives of objective function and non-linear constraints. However, the objective function F_x here may not be able to satisfy this requirement since the absolute value is applied for F_x in equation (11). Another reason is that the objective function may not be able to satisfy the conditions of strictly convexity and each equity or inequity constraint may not be a concave function [18]. Thus, the optimization results would depend on the starting points of variables.

In the current situation, there exist a number of local minima from different starting points since the space with six-design variables is sliced by constraints into many feasible and infeasible regions and there is at least one minimum between any two of six natural frequencies. How to select the starting point to find at maximum probability the global minimum is critical. Tremendous research works have been done in this area due to its complexity and the achievements have been summarized by Pinter [19] up to 1996. All the methods have a certain requirement for the objective function, typically a continuously differentiable function. No method is found to be suitable for the current situation with discontinuously differentiable objective and constraint functions. This drawback can only be overcome by selecting multiple starting points based on the engineering judgement which also suggested by Fonseca [11]. The study is thus carried out to investigate how to select the starting points for each variable so as to lead at maximum probability a global minimum.

At first, a program is developed to carry out optimization with simultaneously selected m_j equidistant points for each variable between their lower bound $\mathbf{a}_l$ and upper bound $\mathbf{a}_u$. For saving computational time, the termination tolerances for variables, objective and constraint functions in the optimization are set at higher values, e.g., 10^{-2} for variables and objective function and 10^{-4} for constraint function, and the evaluation times of objection function for each starting point is limited within 100. The programme will calculate the directional derivative in the search direction and compare it with the tolerances of variables and objective function. The optimization will terminate provided the directional derivative is quite below these tolerances (at least two times below) and all the constraints are satisfied. The optimized results (objective function, variable values at starting points and after optimization) are saved as long as the optimized objective function value is less than that with variables at their lower bound $\mathbf{a}_l$. This implies to search all the solutions better than the conventional engineering design. If the optimized objective function value is found to be the same as anyone saved, its results will be ignored. In the case that the termination tolerances have not been satisfied after 100 times function evaluation, the last optimized results are also saved provided its function value is less than that at lower bounds of variables.

It is applied in the second step for another programme to do optimization at all saved starting points. Since the number of saved points is limited, the termination tolerances for objective and constraint functions in the optimization are reduced down to 10^{-8} and the evaluation times of objection function for each starting point are enlarged to 300 or higher to refine the final minimum from all local minima. This final minimum cannot be guaranteed the global minimum. Theoretically, if m_j is larger enough, the global minimum can be achieved. But the increase of m_j will significantly increase computational time. The following strategies can be applied to reduce the number of the starting points, which comes from the analysis of optimization results: One is to fix the starting point at the lower bound $\mathbf{a}_l$ for the stiffness in one direction if the excitation force in this direction is

significantly larger than that in other directions (>2 times). This can reduce variables from six dimensions to five dimensions. Another one is to select the second starting point of stiffness far from its first starting point at lower bound $\mathbf{a}_l$ since the optimized isolator stiffness always converges to its lower bound as it is near $\mathbf{a}_l$. This can be understood since the isolation system normally has a good performance at the lowest value of stiffness. The last one is to select relatively less starting points for angles since the optimization results are not sensitive to them. The typical values of angles are selected at 0, 45, 90°. It is found that 5–8 starting points for each stiffness and 3 for each angle can obtain a good result. The further increase of points cannot improve much of the final result. This result should be the global value in most cases but not guaranteed.

5. NUMERICAL EXAMPLE

Consider a 4-stroke marine engine with one cylinder that is installed as illustrated in Figure 1. The engine mass is 9600 kg. The mass moment of inertia $I = [I_{xx}\ I_{yy}\ I_{zz}\ I_{xy}\ I_{xz}\ I_{yz}] = [15\,100\ \ 15\,999\ \ 6399\ \ 2000\ \ 900\ \ 1200]$ kg m^2. The damping loss factor η is 0·1.

The forces and moments in Figure 4 are selected as the input force. The engine is supported at four corners by four identical isolators. The location of each mount is listed in the Table 1. Obviously, the c.g. of engine is not at the centre of the geometry of engine block. The lower and upper bounds of isolator stiffness are

$$1{\cdot}92\text{e} + 6\ \text{N/m} \leqslant (K'_x,\ K_y,\ K'_z) \leqslant 3{\cdot}0\text{e} + 8\ \text{N/m}. \tag{25}$$

Based on this lower and upper bounds, the maximum allowable static deflection for an isolator in three directions is 0·0125 m (0·5 in) which is a typical value of neoprene isolator, and the maximum system frequency is about 125 Hz. Bolton-Knight [20] indicated that when an isolator excited at frequencies above 200 Hz, standing waves within the rubber would become significant.

The "dynamic constraint" is set to 0·005 m (0·2 in) which is a typical value of neoprene isolator. With this constraint, the isolator will work within the allowable range of its deflection. In the case the isolator is overloaded in the static equilibrium (the deflection of isolator is over its rated static deflection), the dynamic constraint should be more stringent.

The "frequency constraint" is set to 5 Hz. The main excitation frequencies f_j selected in the "frequency constraint" are 25 and 50 Hz which with most of excitation energy.

The orientation of each isolator is set such that, in each direction, the absolute value of angle of each mount is the same but it may be arranged in the negative direction to satisfy the balance requirement of engine installation. The arrangement of four mount orientations should meet the following equity constraints:

$$-\alpha_1 = \alpha_2 = \alpha_3 = -\alpha_4, \tag{26}$$

$$\beta_1 = \beta_2 = -\beta_3 = -\beta_4, \tag{27}$$

$$\gamma_1 = \gamma_2 = \gamma_3 = \gamma_4, \tag{28}$$

where α_1 means the angle around positive Z-axis at location 1 as shown in Figure 1.

There are totally 24 inequity constraints and 9 equity constraints in this example. The original design is to install isolators under their maximum allowable static deflection

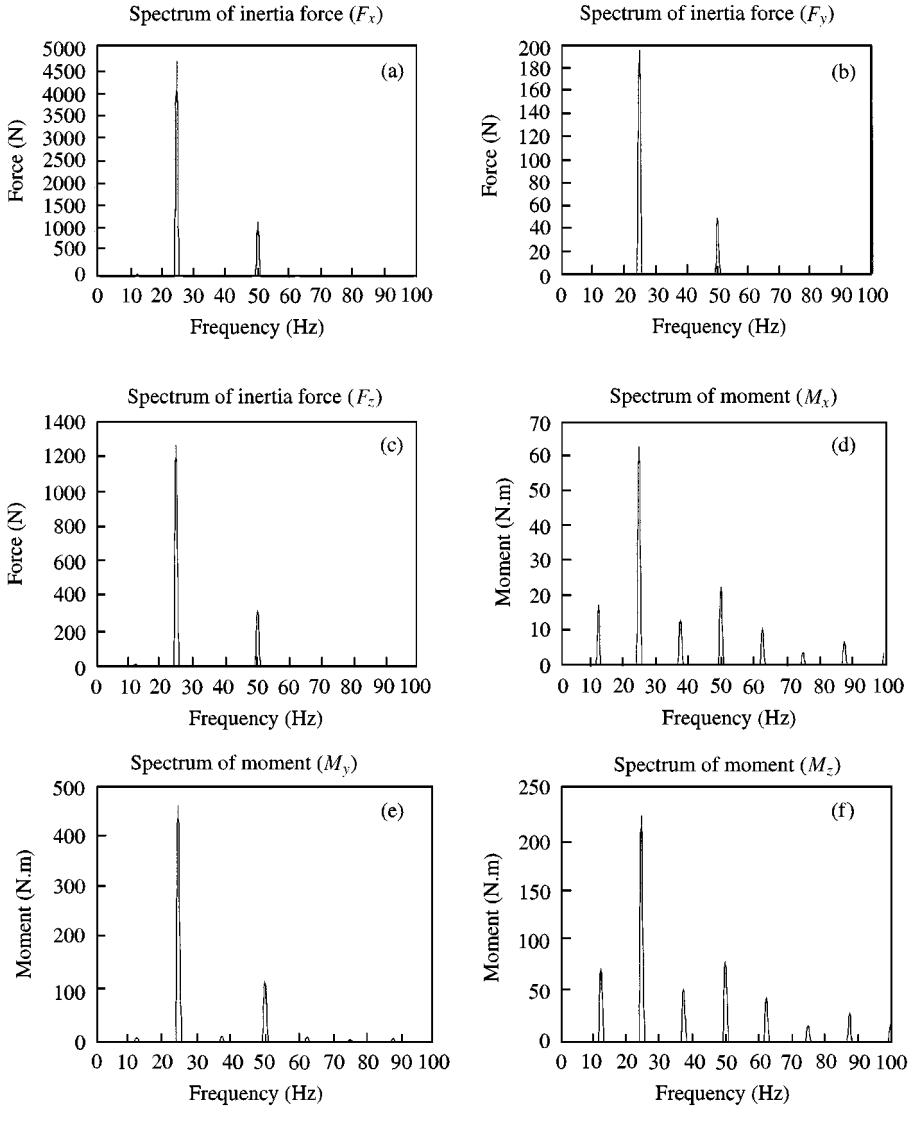

Figure 4. The spectra of the forces and moments after the transformation of the force and moment in Figure 3. The translational displacement of origin of local co-ordinate system is (0·02 m, 0·03 m, 0·1 m) and the rotation angles are (5,10,15) deg.

(0·0125 m) and the isolator's principle elastic directions coincide with the global co-ordinate system ($\alpha, \beta, \gamma = 0$). This is a typical engineering design with the full usage of the potential of isolators.

6. RESULTS AND DISCUSSION

After being optimized, the vertical force transmitted to the base can be reduced to about only half of its original design. Table 2 gives the comparison between the original and

TABLE 1

Mounting locations of isolators

	X(m)	Y(m)	Z(m)
c.g.	0	0	0
Mount 1	− 1	0·8	2·2
Mount 2	− 1	− 1·2	2·2
Mount 3	− 1	− 1·2	− 1·8
Mount 4	− 1	0·8	− 1·8

TABLE 2

Comparison of the objective function and design variables between original and optimized systems

	Original system	Optimized system
Objective function (F_x, N)	212	117
K_x (N/m)	1 920 000	1 920 000
K_y (N/m)	1 920 000	9 460 000
K_z (N/m)	1 920 000	45 300 000
α(Z direction, deg)	0	4
β(Y direction, deg)	0	11
γ(X direction, deg)	0	90

TABLE 3

Comparison of the system natural frequencies between original and optimized systems

Original system natural frequencies (Hz)	Optimized system natural frequencies (Hz)	Excitation frequencies (Hz)
2·9	4·2	12·5
3·8	5	**25**
4·5	5·3	37·5
7·7	13·4	**50**
7·8	32	
9·6	40·4	

optimized systems for objective function, isolator stiffness and mounting orientations. Table 3 gives the comparison of system natural frequencies between the original and optimized systems as well as excitation frequencies. The bolded frequencies are that with main energy of excitation and selected in the "frequency constraint" for optimization. Table 4 gives the comparison between the original and optimized systems for the displacement of engine c.g. It is found from Table 2 that the isolators are selected with higher stiffness in the optimized system. This implies that the high installation deflection in the original system do not mean the higher isolation performance. The careful selection and installation of isolators may get better results even with the lower static deflection. On the

TABLE 4

Comparison of deflection of c.g. of engine between original and optimized systems

Deflection	Original system	Optimized system
x_g (m)	$2{\cdot}24 \times 10e - 5$	$2{\cdot}16 \times 10e - 5$
y_g (m)	$2{\cdot}1 \times 10e - 7$	$2{\cdot}26 \times 10e - 6$
z_g (m)	$6 \times 10e - 6$	$8 \times 10e - 6$
θ_x (deg)	$8{\cdot}6 \times 10e - 5$	$2{\cdot}3 \times 10e - 4$
θ_y (deg)	$1{\cdot}5 \times 10e - 4$	$1{\cdot}3 \times 10e - 4$
θ_z (deg)	$3{\cdot}9 \times 10e - 4$	$1{\cdot}1 \times 10e - 4$

other hand, the reduced static deflection of isolator would also be beneficial to the dynamic balancing of engine mounting system.

The mechanism of optimization was investigated. It can be seen from Table 3 that the isolation improvement in the optimized system is not by moving a natural frequency from an input forcing frequency so as to increase the frequency ratio f/f_0 as stated by Swanson [3] and Spiekermann [2]. This is because the original isolation system has lower system natural frequencies and the higher frequency ratio. From Table 4, it seems that this improvement is achieved by obtaining the larger displacement of c.g. of engine in the Y direction since the value in this direction increases about 10 times. The further investigation is carried out by analyzing the system frequency response with the optimized variables in Table 2. The forces and moments at excitation frequency 25 Hz is selected from all the excitation frequencies as the input force matrix $\{\mathbf{F}\}$ in equation (1) since most of excitation energy is at this frequency. Figure 5 shows the frequency response of original and optimized systems under the same excitation force. It can be seen from Figure 5(a) that the mechanism of vibration isolation of the original system is by moving system natural frequencies quite below the excitation frequencies. This is the conventional design guide for the isolation system. It requires the high static deflection and large allowable dynamic range of movement of isolators and engine block. However, the optimization method is by finding the force dips at excitation frequencies as showed in Figure 5(b). Compared with the force values at 25 Hz in Figure 5(a, b), it is found that the value of optimized system at this frequency is only about 1/4 of the original system. However, this value is about 1/2 (refer to Table 1) for multi-frequencies excitation. It proves that optimization is more effective for a system with a single excitation frequency.

In any constrained optimization, it is important to see which constraints limit the performance of the system. These constraints are called active constraint. Relaxation of these constraints would increase the system isolation performance. On the other hand, the relaxation of other constraints may have no effect on the optimal solution. Table 5 presents the dynamic deflection in three directions at each mount. Since all the values in Table 5 are much lower than the "dynamic constraint" of 5 mm, it is obvious that relaxation of this constraint would have no effect on the system performance. However, the relaxation of "frequency constraint" 5 Hz would have significant impact to the system performance. This impact is shown in Table 6 that the isolation system is optimized with "frequency constraint" at 0, 5 and 10 Hz. The optimized design variables at each case are also given in the table. It is clearly indicated that, without "frequency constraint", the system has the best isolation performance. As "frequency constraint" increases from 5 to 10 Hz, the transmitted force of the optimized systems increases from 117 to 146 N. However, this value only

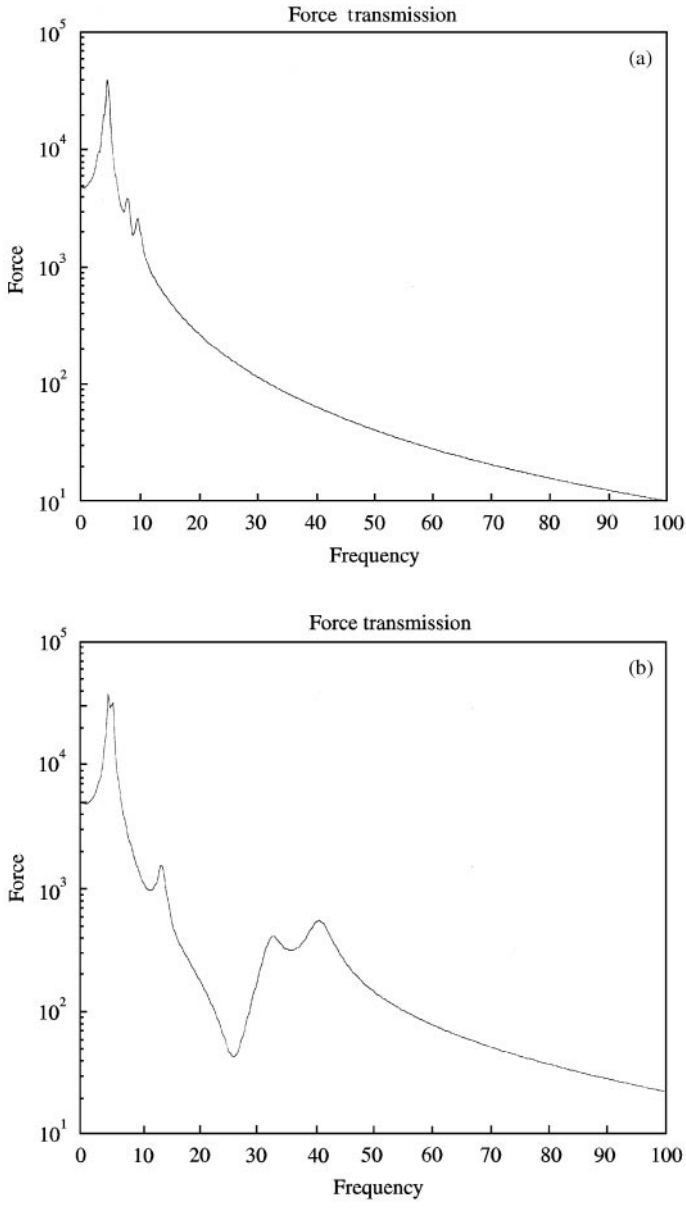

Figure 5. Illustration of the spectra of frequency response of the original (a) and optimized (b) systems. The input force matrix $\{\mathbf{F}\}$ is at 25 Hz with most of energy of excitation.

increases about 3 N as "frequency constraint" varies from 0 to 5 Hz. This implies that "frequency constraint" can be carefully selected to reduce the possibility of system resonance but keep almost the same system isolation performance. As the "frequency constraint" is further increased from 10 Hz, it can be anticipated that the transmitted force also becomes larger and gets close to the value of conventional design (212 N). Another phenomenon found from Table 6 is that, in three cases, K_x, K_y and γ are almost the same after changing "frequency constraint", α and β with small adjustment, but K_z is significantly

TABLE 5

Dynamic deflection in three directions at each mount

	Point 1	Point 2	Point 3	Point 4
U_x (mm)	0·02602	0·02965	0·02063	0·01873
U_y (mm)	0·01167	0·01167	0·00800	0·00800
U_z (mm)	0·00800	0·01540	0·01540	0·00800

TABLE 6

Comparison of the objective function and design variables between optimized systems with different "frequency constraint"

	Optimized system with "frequency constraint" 0 Hz	Optimized system with "frequency constraint" 5 Hz	Optimized system with "frequency constraint" 10 Hz
Objective function (F_x, N)	114	117	145
K_x (N/m)	1 920 000	1 920 000	1 920 000
K_y (N/m)	9 700 000	9 460 000	9 490 000
K_z (N/m)	33 700 000	45 300 000	192 600 000
α	3·6	4	11·6
β	8·8	11	13·8
γ	90	90	90

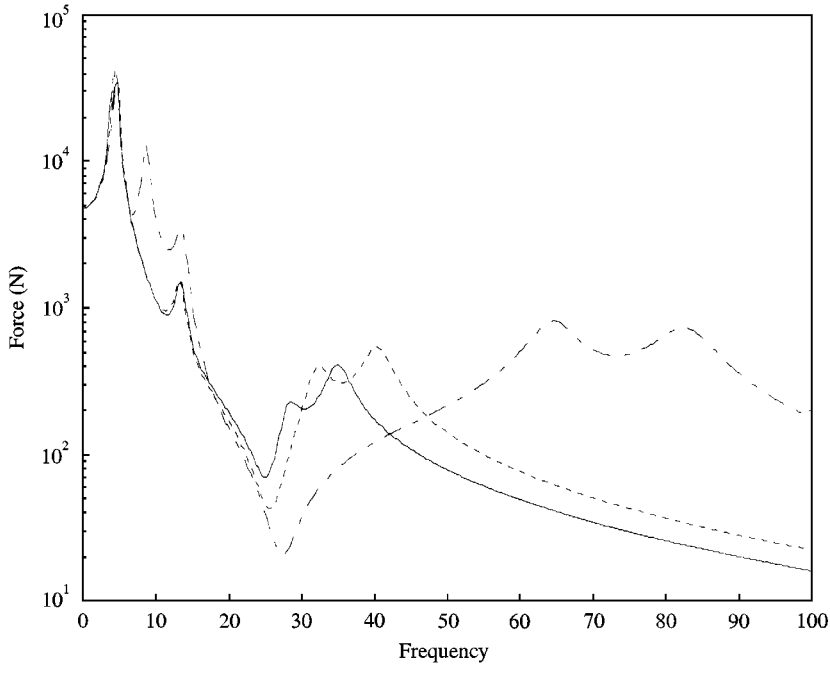

Figure 6. Illustration of the spectra of frequency response of the systems without "frequency constraint" (solid line), 5 Hz "frequency constraint" (dotted line) and 10 Hz "frequency constraint" (dash–dotted line). The input force matrix $\{\mathbf{F}\}$ is at 25 Hz with most of the energy of excitation.

changed. It seems that K_z works as a tuner of the system natural frequency so as to meet the "frequency constraint". Figure 6 illustrates the frequency response of system under three different "frequency constraints". It shows that as "frequency constraint" reduces from 10 to 0 Hz, one of natural frequencies of optimized system will get closer and closer to one of the excitation frequencies (25 Hz). This implies the higher and higher possibility of system resonance. It can thus be concluded that "frequency constraint" should be selected with a compromise between high isolation performance and possible system resonance. It is also interesting to find that, at "frequency constraint" 10 Hz, the transmitted force of optimized system has the lowest value at 25 Hz in Figure 6 but the function value at this "frequency constraint" is the highest in Table 6 as the system has higher force transmission in other excitation frequencies. This implies that the objective to minimize the force transmission at the engine operating frequency (25 Hz at 1500 r.p.m.) does not mean the best design of the isolation system.

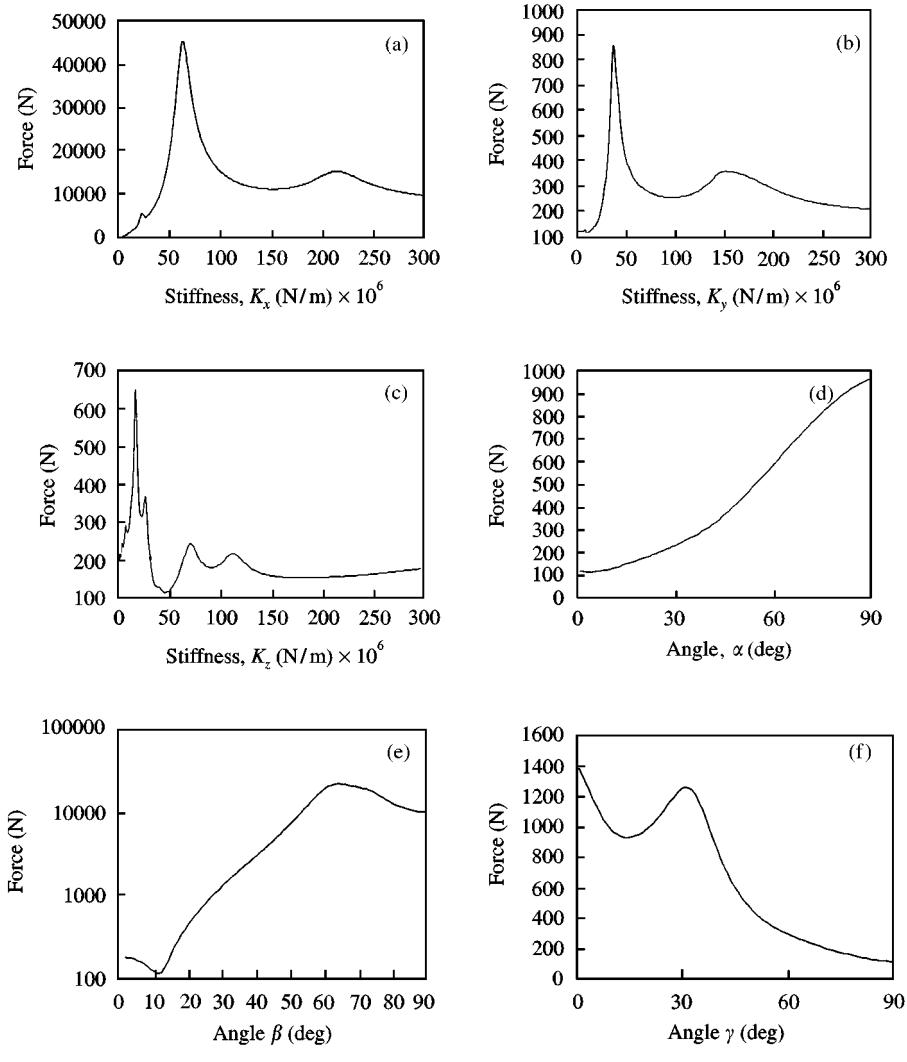

Figure 7. Illustration of system response of one design parameter varying from its lower bound to its upper bound. (a) is with K_x varying, (b) is K_y, (c) is K_z, (d) is α, (e) is β, (f) is γ.

Since SQP method may not be able to find a global minimum, it is necessary to investigate whether there is any other solution that has the lower value of objective function. This has been done by adjusting a design variable from its lower bound to its upper bound while keeping other variables at optimal values. Figure 7(a–f) illustrates the system response at "frequency constraint" 5 Hz to the variation of all design parameters including $K_x, K_y, K_z, \alpha, \beta, \gamma$. It can be seen that the lowest points of objective function are at the optimal values of variables. Figure 7 also illustrates the system sensitivity to the variation of the design parameters. It can be seen from Figure 7 that the objective function is not quite sensitive to the angles but it is sensitive to stiffness. Due to the large scale of horizontal axis (3×10^8), the objective function should not increase too much for a certain percent variation of the stiffness. The calculated force variation is 13 N for 10% change of K_x, 16 N for K_y and 24 N for K_z. It can be anticipated that the relaxation of "frequency constraint" can reduce the force transmission but the force variations above will increase.

7. CONCLUSION

The numerical optimization of a typical 4-stroke engine with one cylinder is presented. The dynamic force in the direction normal to the installation base is minimized. The design parameters are the stiffness coefficients and orientation angles of mounts. Two constraints are imposed in the system. One is to keep the engine static and dynamic deflection within the desired limits. The other one is to set a minimum gap between system natural frequency and engine excitation frequency. The SQP technique has been employed successfully for the optimization. The results of optimization are compared with that of a typical engineering design with the isolators working under their maximum allowable defection. It is found that the transmitted force of the optimized system is significantly reduced. The mechanism of vibration isolation involved in the optimization is investigated with the frequency response of system. It shows that, differing from the traditional isolation system design by shifting the system natural frequencies to lower value, the optimized system is to reduce the force transmission by searching the force dip in the system response to all design variables. The optimization results also indicate that the force transmission for a system with a single excitation frequency is much lower than that for a multi-frequencies excitation. Sensitivity study of the system with the variation of the design parameters is also carried out and it proves that the minimum obtained is the global value in the range of design parameters.

REFERENCES

1. E. Sevin and D. P. Walter 1971 *Optimal Shock and Vibration Isolation*. The Shock and Vibration Information Centre, United States Department of Defence.
2. C. E. Spiekermann, C. J. Radcliffe and E. D. Goodman 1985 *Journal of Mechanisms, Transmissions, and Automation in Design* **107**, 271–276. Optimal design and simulation of vibration isolation system.
3. D. A. Swanson, H. T. Wu and H. Ashrafiuon 1993 *Journal of Aricraft* **30**, 979–984. Optimisation of aircraft engine suspension systems.
4. H. Ashrafliuon 1993 *Journal of Vibration and Acoustics* **115**, 463–467. Design optimisation of aircraft engine-mount systems.
5. J. A. Snyman, P. S. Heuns and P. J. Vermeulen 1995 *Mechanical and Machine Theory* **30**, 109–118. Vibration isolation of a mounted engine through optimisation.
6. C. M. Harris and C. E. Crede 1976 *Shock and Vibration Handbook*. New York: McGraw-Hill, second edition.
7. D. T. Greenwoon 1979 *Principles of Dynamics*. Englewood Cliffs, NJ: Prentice-Hall, second edition.

8. B. PAUL 1979 *Kinematics and Dynamics of Planar Machinery*. Englewood Cliffs, NJ: Prentice-Hall.
9. D. E. GOLDBERG 1989 *Genetic Algorithms in Search, Optimisation and Machine Learning*. New York: Addison-Wesley.
10. K. S. TANG, K. F. MAN, S. KWONG and Q. HE 1996 *Proceedings of the Fourth International Congress on Sound and Vibration. I*, 371–388. Application of genetic algorithms to active noise and vibration control.
11. P. DE FONSECA, P. SAS and H. VAN BRUSSEL 1999 *Journal of Sound and Vibration* **221**, 651–679. A comparative study of methods for optimising sensor and actuator locations in active control application.
12. M. POGU and J. E. SOUZA DE CURSI 1994 *Journal of Global Optimisation* **5**, 159–180. Global optimisation by random perturbation of the gradient method with a fixed parameter.
13. G. N. VANDERPLAATS and H. SUGIMOTO 1985 *Engineering Computations* **2**, 96–100. Application of variable metric methods to structural synthesis.
14. M. J. D. POWELL 1978 *Mathematical Programming* **14**, 224–248. Algorithms for non-linear constraints that use Lagrangian functions.
15. G. J. MOORE 1994 *Design Sensitivity and Optimisation, MSC/Nastran User's guide*, Vol. 68. The Macneal-Schwendler Corp.
16. T. GOLEMAN, M. A. BRANCH and A. GRACE 1999 *Matlab Optimisation Toolbox, User's Guide, Version* 2. The Mathworks Inc.
17. R. FLETCHER 1980 *Practical Methods of Optimisation*. New York: John Wiley and Sons.
18. D. M. HIMMELBLAU 1972 *Applied Nonlinear Programming*. New York: McGraw-Hill.
19. J. D. PINTER 1996 *Global Optimisation in Action*. Dordrecht: Kluwer Academic Publishers.
20. B. L. BOLTON-KNIGHT 1971 *Institution for Mechanical Engineers* **C98**, 24–31. Engine mounts: analytical methods to reduce noise and vibration.